

Active-passive control of portable generator set radiated noise

C.R.Fuller, C.Papenfuss and T.D. Saux

Vibration and Acoustics Laboratories, Virginia Tech, Blacksburg, Virginia, USA

ABSTRACT

This paper summarizes work on applying active and passive noise control to minimize the globally radiated noise of a 2kW portable generator set. The radiated noise of the operating baseline generator set was first measured with a near field microphone array and far field pressure was then estimated using spherical harmonic radiation functions. The spectrum of the radiated noise showed strong tonal characteristics at low frequencies due to the diesel engine making it a good candidate for active noise control (ANC) in that frequency region. However calculations indicated that ANC on its own, while providing high attenuation in the control bandwidth, will lead to only a small reduction in overall A weighted sound pressure levels. Thus passive treatment was applied to control the mid to high frequencies. An optimization technique based upon noise measurements of the passively treated, operating generator set and spherical harmonic radiation functions used in conjunction with a genetic algorithm were used to design the ANC system. The designed ANC system was implemented as a fully integrated, self powered installation into the generator set and the passive and active/passive attenuation in sound measured during operation. The results indicate around 10dBA passive attenuation and additional 5dBA attenuation due to the active system and indicate the performance advantages of an optimally designed ANC system. The work also demonstrates how, in many applications, it is necessary to apply a combined active/passive approach to obtain a wide bandwidth of attenuation and a corresponding significant reduction in overall A weighted sound pressure level.

INTRODUCTION

The operating noise from portable generator sets can be excessive and undesirable due to detection and annoyance issues. The 2 kW Military Tactical Generator(MTG) set shown in Figure 1 was measured to create close to 80dBA at 7 meters distance and 2 meters-head height from the machine. This excessive level is due to engine noise and the open structure of the 2 kW MTG. The operational speed of the MTG is 3600 to 3750 rpm.



Figure 1. Baseline 2kW MTG

In order to increase the utility of the 2kW MTG it is desired to reduce the overall radiated far-field sound levels. A preliminary measurement of the radiated sound at 7 meters was made and an example spectrum is shown in Figure 2. The results show that the noise levels are very tonal and associated with the diesel engine firing order. This is encouraging for active noise control(ANC) as a suitable reference signal can likely be constructed from an engine shaft speed sensor and used in a feedforward control arrangement(Fuller, CR et al, 1996). However the tones can be seen to be significant at mid to high frequencies where ANC is known to be unsuitable. This implies that while ANC might significantly reduce the low frequency levels, the cumulative overall sound levels

are likely to show negligible change due to the mid a high frequency contributions. In addition there are significant tonal levels as low down in frequency as 50 Hz and this is challenging in terms of the required size of active speaker at this frequency. A mandate from the US Army is that any ANC system should fit within the footprint of the baseline machine.

It is also well known that compact, lightweight passive enclosures provide good attenuation at mid and high frequencies but poor attenuation at low frequencies(Bies, D & Hansen, CH, 2002). On the basis of the preliminary baseline testing it was decided that a dual active/passive noise control approach would be pursued which utilizes the advantages of both approach across the complete bandwidth. The ANC system was chosen to provide attenuation in the 0 to 500Hz bandwidth while the passive enclosure system gives attenuation above 500Hz.

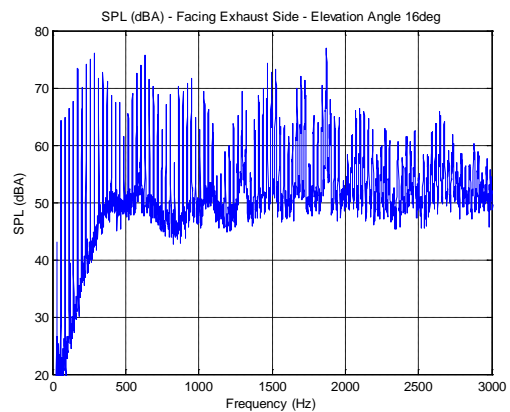


Figure 2. Measured SPL of 2kW MTG at 7 meters, 2 meter height, exhaust side of the machine.

PASSIVE NOISE CONTROL

Accordingly much work was carried out on developing, installing and testing a suitable passive enclosure for the machine. A major requirement for the enclosure is that it provided enough flow of cooling and combustion air to the machine in order not to compromise its operation and also needed to be as lightweight and compact as possible. Figure 3 presents a photograph of the resultant passive enclosure. The sound levels were re-measured at 7 meters and Figure 4 gives example spectra. The results in the top plot show that the passive enclosure gives good attenuations above 300Hz but little below this frequency. The bottom plot is cumulative sound pressure level(SPL) to the frequency of interest and also include ideal ANC over a 0 to 500Hz bandwidth. The bottom plot demonstrates that the overall reduction provided by ideal ANC would be negligible without additional passive treatment.



Figure 3. MTG with passive enclosure under noise testing.

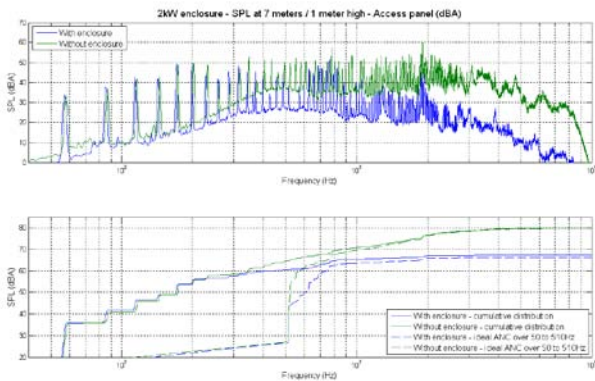
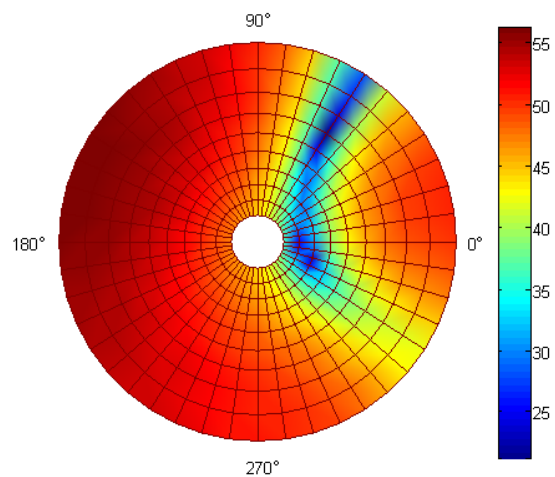


Figure 4. Measured radiated noise with passive enclosure.

INITIAL NOISE MEASUREMENTS

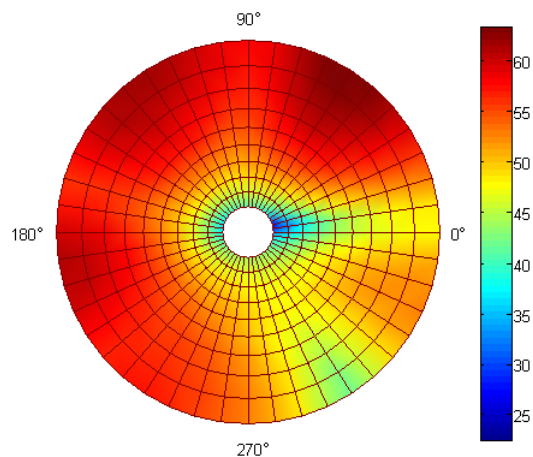
In order to optimally design the ANC system it was necessary to measure the global sound radiation from the machine. Measurements in the far-field at 7 meters would be prohibitive in terms of the number of required transducers and also suffered from signal to noise ratio issues. The procedure used was to measure the radiated sound in the near-field of the machine using the microphone array shown in Figure 3. The generator was located on a flat rotating surface. To obtain a complete hemispherical measurement the generator set was rotated through angular increments until the full 360 degrees was covered. The near field measured sound was then “propagated” to the far-field using radiation functions based upon half space spherical radiation harmonic expansion terms. More details on the theory behind this technique is presented in (Fuller CR et al, 2009 and Rafaely, B, 2005).

Figures 5 and 6 shows two example global sound radiation plots at 7 meters from the generator set for 141 Hz and 226Hz which are harmonic tones of the radiated noise. The exhaust outlet of the machine is in the 180 degree direction. The contour plots are looking down at the hemisphere surrounding the generator set. Figure 5 reveals that, even at 141Hz where the wavelength is 2.43 meters and thus much larger than the machine, diffraction and shadowing effects occur on the side of the machine away from the exhaust outlet. Thus the radiation of the machine is quite complex and distributed in nature and this necessitates an automatic optimal design approach to locating the active sources. Initially it was thought that a heuristic approach of locating the active source close to the loudest noise source of the exhaust outlet would suffice but testing proved this to not be the case(Fuller, CR et al, 2009). In order to achieve significant global ANC attenuation, an optimal design approach was proved to be required.



Radiation pattern (SPL dBA) - 2kW generator enclosure -141Hz

Figure 5. Radiated sound levels at 7meters, 141Hz.



Radiation pattern (SPL dBA) - 2kW generator enclosure -226Hz

Figure 6. Radiated sound levels at 7meters, 226Hz.

ANC SYSTEM OPTIMAL DESIGN

An optimal design approach was developed which used a combination of the measured sound signals at 7 meters(discussed in the previous section) in conjunction with Boundary Element Models(BEM) of the radiation from the active speakers. The BEM models of the various active

speakers used in the implementation(see below) included the speaker housing, diffraction around the passive enclosure of the generator set and were validated by testing in the VT anechoic chamber. Since, in the iterative optimal design approach discussed below, the position of the active speaker will change, a coordinate transformation approach was utilized to find the different radiation from the active source(s) at differing positions on the enclosure but radiating to a fixed observation point in space.

The optimal design approach is shown schematically in Figure 7 and is an iterative approach based upon Genetic Algorithms(GA). The fitness function is the summed squared error between the measured complex valued generator noise field and the complex valued BEM calculated noise field due to the active sources. The error is summed over at a number of discrete points on a hemisphere surrounding the machine at 7 meters to form the fitness function (similar to an ANC cost function). Certain variables have to be specified a priori. These are the number of active sources, the bandwidth over which each active source is to provide ANC and areas on the housing where it is not possible to locate the active sources(optimization constraints). The GA starts by utilizing randomly selected locations of the active sources and following the procedure of Figure 7 until the fitness function does not reduce significantly with further iterations(has converged).

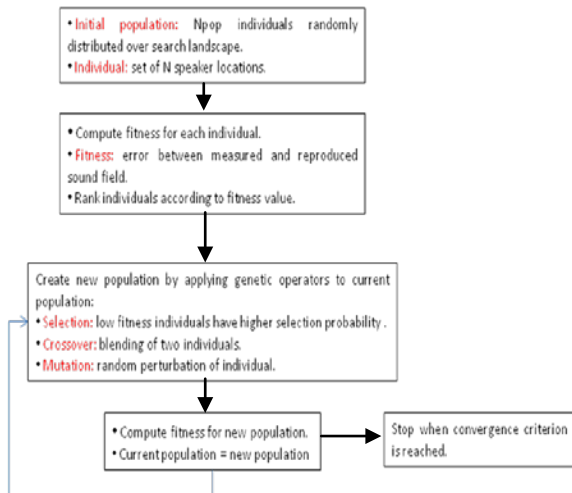


Figure 7. ANC system optimization approach based on Genetic Algorithms.

The optimal positions of the active sources found using the above approach are shown in Figure 8. For this optimal design four active sources were employed; a subwoofer designed to work over the 60 to 200Hz bandwidth and three woofers designed to work over the 150 to 500Hz bandwidth. The control bandwidth was set at 50 to 500Hz. It is interesting that the subwoofer is not located near the engine exhaust outlet which was measured to be the loudest noise source and the other active speakers are distributed around the enclosure. This indicates that the sound radiation not only comes from the exhaust outlet but also from the body of the enclosure panels. The vibration of the panels is small but their area is large, thus resulting in a significant volume velocity source.

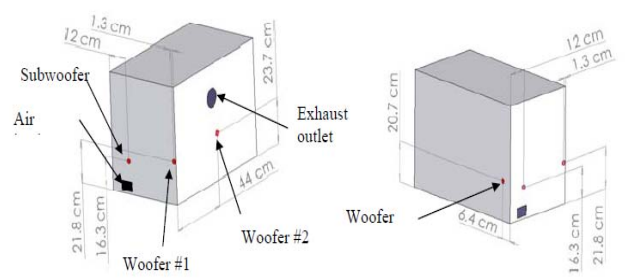


Figure 8. Optimal locations of the active sources.

Figures 9 and 10 give the predicted ANC overall reduction, at 7 meters, summed over the control bandwidth for elevations of 4 degrees and 12 degrees. Attenuations of up to 15dBA are apparent in selected directions. The corresponding overall attenuation summed over the hemisphere was calculated to be 8dBA.

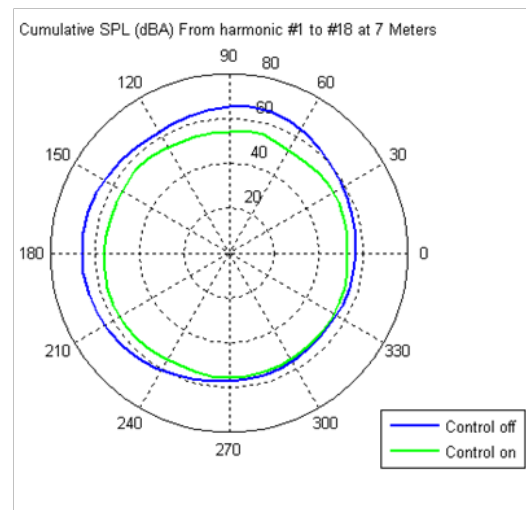


Figure 9. Predicted ANC performance for optimal design, 4 degree elevation.

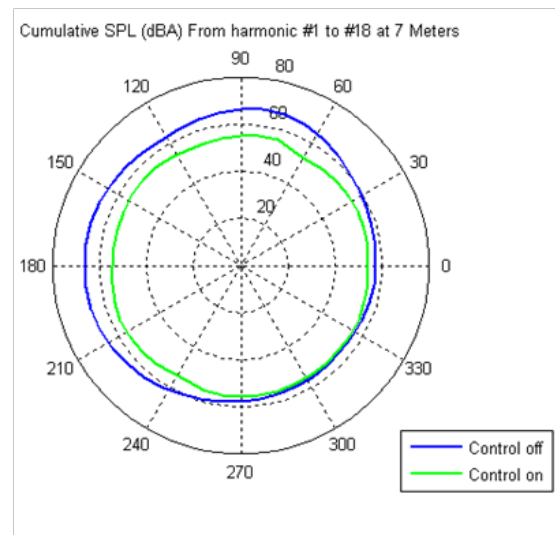


Figure 10. Predicted ANC performance for optimal design, 12 degree elevation.

ANC SYSTEM IMPLEMENTATION

The various components of the ANC system are the active sources, the control module including reference signal generation, power electronics, error sensors and conditioning electronics. We now briefly discuss implementation of each of these components.

Active speakers

As well as providing the predicted ANC performance, the optimal design procedure also allowed the calculation of the required active source volume velocity to achieve control over the actual, measured radiated sound levels from the generator set. These calculated values then allowed estimation of the required SPL at 1 meter which is the standard metric of specification for baffled speakers. Using this approach the speakers outlined in Figure 11 below were chosen for the active system. Their measured response in given in Figure 12. These values were measured in the VT anechoic chamber with the speakers installed in the walls of the generator enclosure with speaker enclosures.

	Subwoofer: Earthquake audio SWS-8	Woofer: Dayton ND140-4
Mounting depth	2-1/8"	2-1/2"
Cutout diameter	8-1/8"	4-3/4"
Vas	17.2 liters	10.2 liters
Q factor	2.652	1.043
Sensitivity	86.7dB 1Watt/1meter	85.3dB 1Watt/1meter
-3dB cutoff frequency (predicted)	63Hz (in 3 liters sealed enclosure)	92Hz (in 2 liters sealed enclosure)
Resonance frequency (predicted)	99Hz (in 3 liters sealed enclosure)	148Hz (in 2 liters sealed enclosure)

Figure 11. Specifications of chosen active speakers.

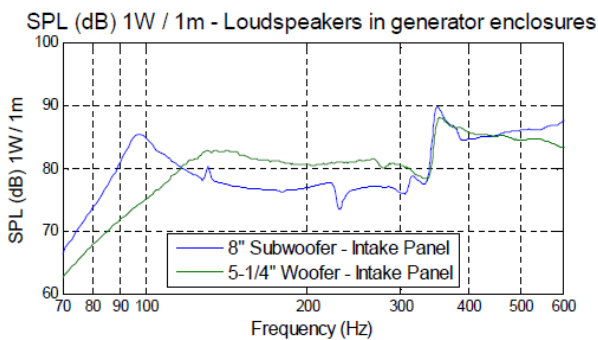


Figure 12. Measured performance of chosen active speakers in the VT anechoic chamber.

An example of the active speakers installed in the intake panel of the enclosure including the speaker enclosures is given in Figure 13. Care must be taken to design the speaker enclosure so that the speakers do not impinge on the generator baseline equipment or interfere with air cooling flow.

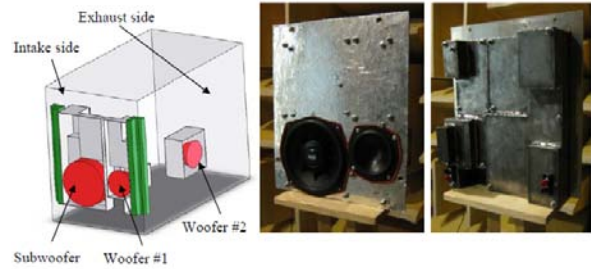


Figure 13. Active speakers installed in intake panel.

Control module

The control module is the heart of the ANC system and contains the Digital Signal Processor(DSP), analog to digital converters(ADC), digital to analog converters(DAC), anti-aliasing filters, smoothing filters, power electronics and sensor power and conditioning electronics. Since a mandate was to implement a stand alone ANC system within the foot print of the generator set it was necessary to integrate all of the above components into a single module shown in Figure 14. The DSP system is programmable by a removable set up cable connected to a lap top PC. The control code and operating parameters were downloaded into the control module and the controller performance monitored during system testing and optimization runs. Once the controller was optimized, the set up cable was removed and the control module set to run in autonomous mode. In this mode, once switched on, the control code went through an initialization phase, a system identification phase and an adaption phase. For testing a toggle switch activated by a long cable was installed to facilitate on-off testing of the ANC system. The module was also self powered by the output of the generator set thus the ANC system was completely stand alone and fully integrated into the machine.

The control code utilized was the standard digital time domain Filtered X LMS algorithm(Fuller, CR et al, 1996) implemented in a 4I4O arrangement. In this implementation the reference signal was also generated on the DSP using an electrical signal from the actual generator output. This signal was processed and used to digitally generate a series of discrete tones corresponding to the diesel engine firing order(shown in Figure 2). Since the electrical generator is hard connected to the diesel engine, the reference signal is thus highly correlated with the sounds radiated at the generator set tones. A block diagram of the control system is shown in Figure 15.

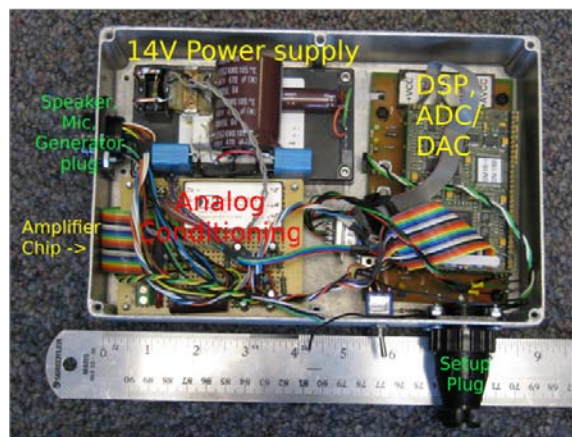


Figure 14. ANC control module.

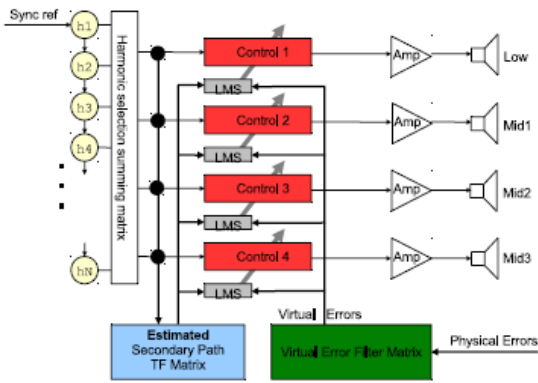


Figure 15. Controller block diagram.

Virtual error sensors

Most ANC systems utilize error sensors located in the zone where cancellation is required. However for the portable generator set locating error microphones at 7 meters from the machine is impracticable and other error sensor strategies have to be employed. For this application we utilized “virtual error” sensor technology(Garcia-Bonito, J et al,1996) where signals from sensors located locally on the machine are processed in order to provide a signal for “virtual” sensors located at 7 meters from the machine. A block diagram of the process is shown in Figure 16. For this configuration, four microphones are located on each four side panels of the machine. A set of four microphones were temporarily located in the far-field at 7 meters in each quadrant of the radiation field(the points where ANC reduction is required). Without the generator running, white noise was played through the active speakers and the LMS algorithm is used to estimate the filters F_{MkN} . These coefficients were stored in the DSP as shown in Figure 15 for use of the ANC system without far-field microphones. Once the virtual error sensor system was implemented the ANC system(designed to provide far-field reduction at 7 meters) could be operated without far-field microphones in place. Note this approach only optimizes the virtual error sensors for the active source outputs and not the generator set radiated noise. A higher order virtual sensor would model both radiation sources but require more filters.

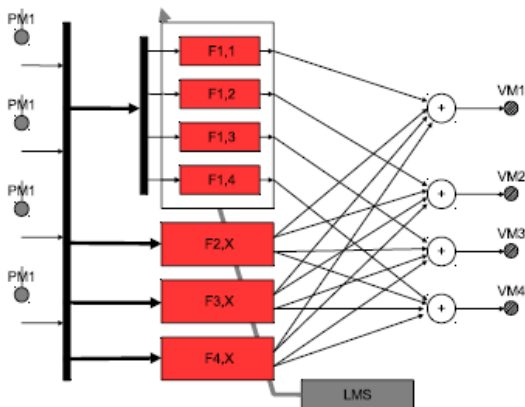


Figure 16. Virtual error sensor process block diagram.

ANC SYSTEM FIELD TESTING

The performance of the ANC system was ultimately evaluated in field testing in order to replicate a realistic application. Figure 17 is a photograph of the generator set ANC system undergoing testing in a field outside of Blacksburg, Virginia.



Figure 17. Field testing of the ANC system.

The generator set was centrally located in an array of 12 monitor microphones located at 7 meters, 2 meters/head height (US Army standard test procedure) and used to measure the overall radiation from the machine under the various test conditions. The control module was programmed with the download cable connected to a PC and then removed. The signals from the microphones were acquired using a multi-channel data acquisition (DAQ)system. The instrumentation, PC and DAQ are shown in Figure 17. A long cable and switch was used to turn the ANC system on and off for different measurement scenarios. Here we present the results for ANC performance using (i) four physical error microphones located in the far-field at 7 meters and in each quadrant and (ii) virtual error sensors located on the machine to represent the physical microphones as discussed above.

Figure 18 presents the control bandwidth ANC performance results for physical error sensors. The results are presented for each quadrant of the far-field radiation. Both narrowband and cumulative SPL(dBA) are presented. The results show impressive ANC reduction in the far-field of between 3.5 and 11dBA. The highest attenuations occur in the radiation directions where the sound levels are highest. The cumulative SPL reveals that the ANC system is not providing any attenuation below 80Hz and this is due to limitations on the output of the active subwoofer below this frequency. A more efficient subwoofer would lead to even greater ANC reduction over the control bandwidth. Figure 19 is a radiation directivity plot corresponding to results of Figure 18. Impressive global reductions are apparent.

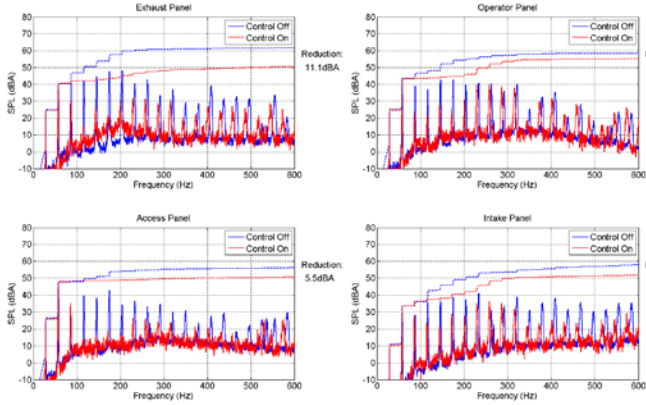


Figure 18. ANC performance over control bandwidth, physical error sensors.

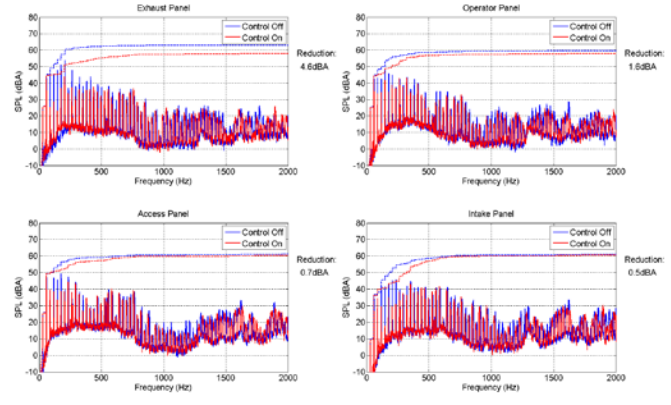


Figure 20. ANC performance over control bandwidth, virtual error sensors.

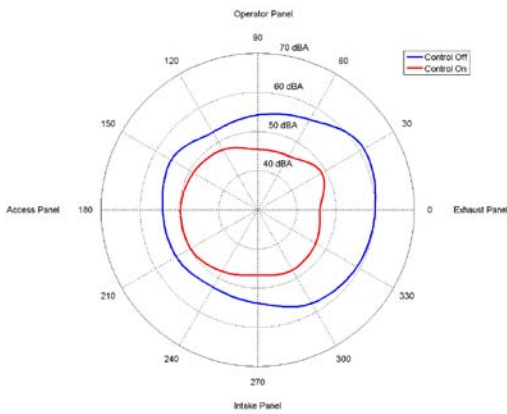


Figure 19. Directivity plot for results of Figure 18.

Figure 21 presents the directivity plots at 7 meters corresponding to the results of Figure 20. The levels are overall SPL (dBA) summed over the complete bandwidth of 0 to 2000Hz. Global reductions are again evident.

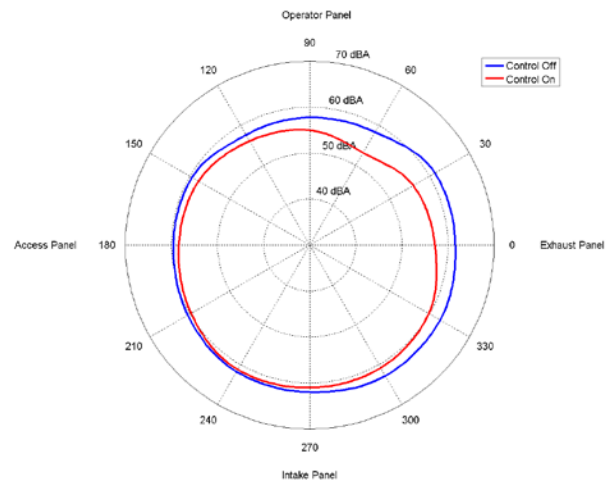


Figure 21. Directivity plot for results of Figure 20.

We now turn to example results for the ANC performance with virtual error sensors. Figure 20 shows the spectra in each quadrant measured at the monitor microphone array when virtual error sensor technology is utilized. For these results the spectra are presented for full bandwidth of 0 to 2000Hz. The overall levels are thus similar to what would be perceived in a subjective test. The ANC system with virtual error sensors is demonstrated to provide overall reductions of between 0.5 to 4.6dBA. The highest attenuations again occur in the directions of loudest sound radiation which is a characteristic of the LMS control algorithm(Fuller, CR et al, 1996). An examination of the cumulative SPL reveals that the ANC system provides very good attenuation over the control bandwidth of 0 to 500Hz. The overall attenuation is therefore limited by the contributions of mid frequency tones which are out of the control bandwidth.

We now summarize the results utilizing spectral plots of cumulative SPL in dBA shown in Figure 22. The results are for an ANC system with virtual error microphones. The performance was again measured using physical microphones located at 7 meters from the machine. In the results of Figure 22 sound levels are given for (i) baseline machine (ii) passive treatment and (iii) active-passive treatment. The results reveal that the passive treatment is effective above approximately 300Hz and provides very little attenuation below that frequency. The ANC system on the other hand can be seen to be effective between 80 to 500Hz and provides negligible attenuation above that frequency. The combination of active-passive treatment which provides full bandwidth attenuation can be seen to be very effective over the complete frequency range providing overall attenuations of between 10.5 to 13dBA reduction. It should be noted that the ANC performance achieved with the optimally designed system far-exceeded that achieved with a heuristically designed ANC system studied in previous work on a similar machine(Fuller,

CR et al, 2009). This observation highlights the advantage of optimal design methods when the radiation field has complexities such as shown in Figure 5, even at low frequencies when the wavelength is much longer than the source size.

Rafaely, B, 2005, 'Analysis and Design of Spherical Microphone Arrays', Proceedings of IEEE Transactions on Speech and Audio Processing, Vol. 13(1), pp.15-143.

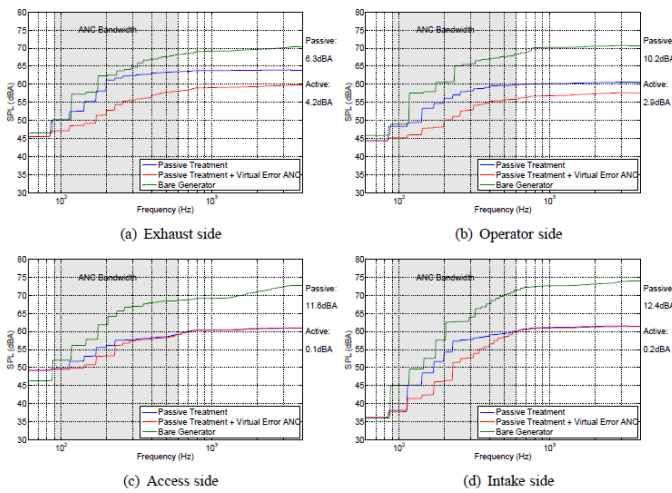


Figure 22. Summary results for active-passive treatment of generator set radiated noise, ANC system utilizing virtual error sensors.

CONCLUSIONS

An active-passive system for reducing sound radiated from a 2kW portable generator set has been optimally designed, implemented and field tested. The ANC system includes virtual error sensor technology in which error microphones located in the far-field are replaced with microphones located on the generator enclosure and signal processing. The field testing demonstrates that the active-passive system can provide very high attenuations in overall SPL (dBA) of the order of 10 to 13 dBA. The work also shows the efficiency of utilizing a combined active-passive approach where the ANC system is configured to function in the low frequencies while the passive system functions in the mid to high frequencies thus providing full bandwidth control. The work also illustrates the performance advantage of utilizing an automatic approach for optimal design of the ANC system based upon a discrete optimization approach. Levels of attenuation performance achieved with the optimally designed system far exceeded those achieved with a heuristically designed system thus illustrating the complexity of the radiation field from the generator set even at very low frequencies.

REFERENCES

- Bies, DA & Hansen, CH, 2002, *Engineering Noise Control*, Spon Press, London
- Fuller, CR, Elliott, SE & Nelson, PA, 1996, *Active Control of Vibration*, Academic Press, London.
- Fuller, CR, Papenfuss, C & Saux, TD, 2009, 'Active Control of Portable Generator Set Noise; Heuristic versus Design', Proceedings of ACTIVE 2009, Ottawa, Canada.
- Garcia-Bonito, J, Elliott, SJ and Boucher, CC, 1996, 'A Virtual Microphone Arrangement in a Practical Active Headrest', Proceedings of INTERNOISE 96, Liverpool, UK.